Journal of Materials Chemistry B

Accepted Manuscript

ROYAL SOCIETY OF CHEMISTRY

www.rsc.org/materialsB

Journal of Materials Chemistry B RSCPublishing

PAPER

Enhanced bone regeneration with a gold nanoparticle-hydrogel complex

Cite this: DOI: 10.1039/x0xx00000x

Dong Nyoung Heo,[a] Wan-Kyu Ko,[a] Min Soo Bae,[a] Jung Bok Lee,[a] Deok-Won Lee,[b] Wook Byun,[a] Chang Hoon Lee,[c] Eun-Cheol Kim,[d] Bock-Young Jung*[e] and Il Keun Kwon*[a]

Received ooth January 2012,
Accepted ooth January 2012

DOI: 10.1039/x0xx00000x

www.rsc.org/MaterialsB

Gold nanoparticles (GNPs) are widely used in diagnostics, drug delivery, biomedical imaging, and photo-thermal therapy due to their surface plasmon resonance, fluorescence, and easy-surface functionalization. According to recent studies, GNPs display a positive effect on the osteogenic differentiation of mesenchymal stem cells (MSCs) and MC3T3-E1 osteoblast-like cells. The aim of this study was to develop a new approach for bone tissue regeneration based on the utilization of biodegradable hydrogel loaded with GNPs. We have used photo-curable gelatin hydrogels (Gel) in order to provide a proof of principle of GNPs in regeneration strategies for bone tissue repair. We have investigated the effects of these Gel-GNP composite hydrogels both *in vitro* and *in vivo*. The *in vitro* results showed that the hydrogels loaded with GNPs promote proliferation, differentiation, and alkaline phosphate (ALP) activities of human adipose-derived stem cells (ADSCs) as they differentiate towards osteoblast cells in dose-dependent manner. Moreover, the *in vivo* results showed that these hydrogels loaded with a high concentrations of GNPs had a significant influence on new bone formation. Through these *in vitro* and *vivo* tests, we found that the Gel-GNP can be a useful material for bone tissue engineering.

Introduction

Biodegradable hydrogels containing colloidal nanoparticles have been actively studied for applications in the biomedical and biotechnological fields for many years.[1-3] Recently, there has been a great deal of research focusing on the development of hybrid biomaterials composed of hydrogels and inorganic nanoparticles.[4-6] Inorganic nanoparticles embedded into polymeric hydrogels are an effective method for enhancing the functionality of the nanoparticles in biological systems. Such a hybrid material also presents a double advantage of having the properties of both the hydrogel and the nanoparticles.

Various protein-based polymers, such as collagen, gelatin, fibrin, silk fibroin, and elastin, have attracted particular attention for their potential applications as hydrogels. This is due to their capacity to mimic many of the features of extracellular matrix.[7,8] Among these various materials, gelatin was selected as a means to prepare hydrogels due to its many advantages of biodegradability, biocompatibility, and non-toxicity. Gelatin is a hydrolysis product of collagen derived from connective tissues such as skin, bone, cartilage, and tendons of animals.[9,10] Therefore, it maintains many bioactive features of collagen.

In parallel, developments of nanotechnology in the past few decades have demonstrated the application of gold nanoparticles (GNPs) towards drug delivery, cell targeting, bio-sensing, and tissue engineering.[11,12] In the biomedical field, GNPs are very attractive materials because of their potential use in a broad range of applications due to their unique physical and chemical properties.[13,14] In recent years, GNPs have been reported to be a new generation of osteogenic agents for bone tissue regeneration.[15,16] It has been demonstrated that GNPs promote osteogenic differentiation of mesenchymal stem cells (MSCs) after intracellular uptake through activating the p38 mitogen-activated protein kinase (MAPK) pathway.[15] Dan *et al.* described that GNPs with diameters of both 20 and 40 nm lead to an increase in the osteogenic differentiation rate of MC3T3-E1 osteoblast-like cells.[16] Furthermore, GNPs can affect osteoclast formation. Sul et al. showed that GNPs inhibit the receptor activator of nuclear factor-κb ligand pathway towards osteoclast formation in bone marrow-derived macrophages.[17]

One of the strategies for improving bone tissue regeneration is to enhance the osteogenic differentiation of osteo-progenitor

[a]*Department of Maxillofacial Biomedical Engineering and Institute of Oral Biology, School of Dentistry, Kyung Hee University, Seoul 130-701, Republic of Korea. Email: kwoni@khu.ac.kr*
[b]*Department of Oral and Maxillofacial Surgery, Kyung Hee University Dental Hospital at Gang-dong, Seoul 134-727, Republic of Korea*
[c]*Department of Oriental Gynecology, College of Oriental Medicine, Kyung Hee University, Seoul 130-701, Republic of Korea*
[d]*Department of Maxillofacial Tissue Regeneration and Research Center for Tooth and Periodontal Regeneration (MRC), School of Dentistry, Kyung Hee University, Seoul 130-701, Republic of Korea*
[e]*Deptartment of Advanced General Dentistry, College of Dentistry, Yonsei University, Seoul 120-752, Republic of Korea. Email: JBY1004@yuhs.ac*

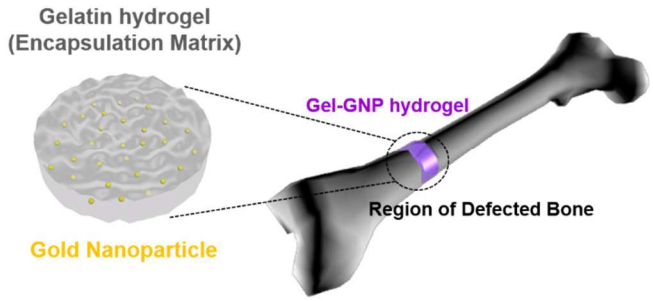

Fig. 1 Schematic diagram of photo-cured gelatin hydrogel network loaded with GNP and its application for treating bone defects.

cells by osteo-inductive agents. It is well known and recognized that bone morphogenic proteins (BMPs) has beneficial effects on bone regeneration and repair.[2,3,18] Although BMPs are effective agents in enhancing bone tissue regeneration, the clinical utility is limited by certain disadvantage, such as excessive cost, unwanted bone formation, and local inflammatory reaction.[19-21] Therefore, it is necessary the development of alternative agents to provide less expensive, more safer, and effective properties. In the previous studies, the effect of gold nanoparticles as osteogenic agents were well-described. The GNPs would be suitable materials in accord with above mentioned factors. However, previous researches just confirmed about their osteogenic effects at *in vitro* condition. Although the effects of GNPs in the osteogenic differentiation is evident at *in vitro*, the interactions between GNPs and bone tissues have not been studied. The results of *in vitro* may not always be the same as that of *in vivo*. Therefore, *in vivo* studies need to check the osteogenic effects of GNPs. In view of the importance of the above works, we have fabricated a hybrid hydrogel composed of gelatin and GNPs as a means to enhance bone tissue regeneration (Fig. 1). The hybrid hydrogel was formed by irradiating a mixture of a photo-initiator, methacrylated gelatin (GelMA) and GNPs with ultraviolet (UV) light. The content and distribution of GNPs in the GelMA solution and hydrogel were determined by UV/Vis spectroscopy, differential scanning calorimetry (DSC) and thermo-gravimetric analysis (TGA). The GNPs embedded in a gelatin hydrogel were evaluated for their capacity to induce osteogenic differentiation of human adipose-derived stem cells (ADSCs). ADSCs are excellent multi-potent stem cells that are capable of differentiating into several types of cells such as osteoblasts, adipocytes, chondrocytes, and myoblasts.[22,23] The effectiveness of these hybrid hydrogels for treating bone defects was evaluated under *in vivo* conditions.

Experimental section

Materials

The chemicals used in the synthesis of methacrylated gelatin (GelMA) [Gelatin derived from porcine skin (type A), methacrylic anhydride (MA)] and the production of gold nanoparticles (GNPs) [chloroauric acid ($HAuCl_4$), trisodium citrate] were purchased from Sigma-Aldrich (St. Louis, MO, USA). Photo-initiator, 1-[4-(2-hydroxyethoxy)-phenyl]-2-hydroxy-2-methyl-1-propanone (Irgacure 2959) for photopolymerization was purchased from Ciba Specialty Chemicals (Basel, Switzerland). Human Adipose-Derived Stem Cells (ADSC), MesenPRO RS™ medium supplemented with MesenPRO RS™ growth supplement, alpha-minimum essential medium (α-MEM), fetal bovine serum (FBS), dulbecco's phosphate-buffered saline (DPBS), trypsin–EDTA and penicillin–streptomycin (PS) were purchased from GIBCO BRL (Invitrogen Co., USA). Bone morphogenetic protein-2 (BMP-2) was purchased from R&D Systems (Minneapolis, MN, USA). All reagents were used as received without further purification.

Equipment

Transmission electron microscopy (TEM) observations were carried out using an H-7100 (Hitachi, Japan). Dynamic light scattering (DLS) measurements were carried out using a 90 PLUS (Brookhaven, USA). Ultraviolet/Vis absorbance (UV/Vis) was measured using an UV-1650PC (Shimadzu, Japan) spectrophotometer. Wide angle X-ray diffraction measurements were carried out using a D8 Advance (Bruker, USA) diffractometer. Thermal analyses such as differential scanning calorimetry (DSC) and thermogravimetric analysis (TGA) were measured using SDT Q 6000 (TA Instruments, USA), at a heating rate of 10 °C/ min under a constant nitrogen flow.

Synthesis of GelMA

GelMA was synthesized as described previously.[24-26] Briefly, gelatin was dissolved in DPBS at 50 °C to make a 10 wt.% uniform solution. A high degree of methacrylation was achieved by adding 20% (v/v) of MA to the synthesis reaction. MA was added to the gelatin solution at a rate of 0.5 ml/min under stirring conditions. The mixture was allowed to react at 50 °C for 3 h. After a 5× dilution with additional warm DPBS, the GelMA solution was dialyzed against deionized water using a 12–14 kDa cutoff dialysis tube for 6 days at 40 °C to remove unreacted MA and other impurities. The GelMA solution was frozen at -80 °C, lyophilized and stored at -80 °C until further use.

Preparation of Gel-GNP composite hydrogels

Aqueous solutions of GNP were synthesized by citrate reduction of $HAuCl_4$.[27] Briefly, 0.5 mM $HAuCl_4$ (800 mL) solution was refluxed, and then 2% trisodium citrate (15 mL) was quickly added. After 15 minutes, the color of the solution changed to dark red, followed by the formation of GNP. The GNP solution was used without further purification in all experiments. The Gel-GNP composite hydrogels were prepared by UV-induced chemical crosslinking. Briefly, a series of varying dilutions of GNPs (final concentration 1, 5 and 14 μg in 70 μl) were mixed with 10% (w/v) GelMA and 0.1% (w/v) photo-initiator. Subsequently, 70 μl of these mixed solutions were pipetted between two glass slides separated by a 500 um spacer and exposed to UV light (320–500 nm, 7.0 mW / cm^2, EXFO Omnicure S2000) for 60 sec. Samples (12 mm in diameter and 500 um in height) were detached from the slides and incubated in DPBS at 37 °C for 24 h and used for further experiments. In this study, these are designated as Gel-GNP **1** (1μg), **2** (5 μg) and **3** (14 μg) for each dilution level of GNPs. To compare the functionality of the GNPs, 10 ng of functional factor, BMP-2 of amounts used in previous study, was added in the mixed solution with 70 μl of 10% (w/v) GelMA and 0.1%

(w/v) photo-initiator (Gel-BMP) and photo-polymerized by UV light.[28]

In vitro enzymatic degradation

To characterize the enzymatic degradation properties of Gel–GNP hydrogels, each hydrogel sample was placed in a 1.5 ml centrifuge tube and incubated with 1 ml of collagenase solution (2.5 U ml^{-1}, collagenase type II) at 37 °C. At the predefined time points, the hydrogel was removed, frozen and lyophilized. The percent degradation was calculated by the ratio of the final weight to the original weight. The sample size was five gels per group.

The morphology of the degraded hydrogel was determined by labelling with an amine reactive fluorescent dye (Alexa Fluor 488 carboxylic acid, succinimidyl ester, Molecular Probes®) to facilitate visualization. Briefly, the dye was dissolved in dimethyl sulfoxide (DMSO) at a concentration of 0.5 mg/ml. This stock solution was then diluted with sodium bicarbonate (50 mM, pH 8.5) to obtain a working concentration of 50 μg/ml. The sample was then soaked in 1 ml of working solution for 1 h at the room temperature, and rinsed three times in DPBS. The fluorescently labeled hydrogel was imaged by confocal laser scanning microscopy (CLSM, Eclipse E600W, Nikon, Tokyo, Japan). The obtained images were assayed by using Nikon EZ-C1 software.

Cell culture

ADSCs were used to study cell cytotoxicity and osteogenic differentiation. ADSCs were cultured in a standard cell culture incubator under a humidified atmosphere with 5% CO_2 at 37 °C. The cells were maintained in MesenPRO RS™ medium supplemented with MesenPRO RS™ growth supplement, 2% FBS, and 2 mM glutamine. The media was changed every 3 days. All cells were used when they were in exponential growth phase. For biological experiments and analyses, the cells were harvested, collected by centrifugation at 1,000 rpm for 5 minutes, and then seeded in well plates prior to *in vitro* biological evaluation. For *in vitro* studies, hydrogels (12 mm in diameter and 500 um in height) were prepared on 3-(trimethoxysilyl)propyl methacrylate (TMSPMA)-coated glass slides by UV-induced chemical crosslinking. The cross-linked hydrogels for each Gel, Gel-BMP, Gel-GNP**1**, **2**, and **3** were then prepared and placed in DMEM at 37°C overnight.

Cell proliferation and viability

ADSCs were detached from the culture dishes using trypsin–EDTA solution and seeded on the various kinds of hydrogels at a density of 5×10^4 cells. The cell proliferation of the hydrogels was evaluated by using a cell counting kit (CCK-8, Dojindo Molecular Technologies Inc., Japan). After seeding the cells, adhered and proliferate cells were measured at 24, 48, and 72 h. At each predetermined time point, hydrogels were washed with DPBS, and a fresh medium containing CCK-8 (300 μl of 0.1 ml/ml) was added. This was then incubated for 2 h and the intensity was measured by a microplate reader (BioRad, USA) at a wavelength of 450 nm. Additionally, cell viability was evaluated by using a calcein-AM/ethidium homodimer-1 (EthD-1) live/dead assay kit (Invitrogen, USA). After 24 h of incubation, cell-seeded hydrogels were rinsed with DPBS and the test solution of 2 μM calcein AM and 4 μM EthD-1 was added directly to each hydrogels. Afterward the stained cells were observed by CLSM.

Alkaline phosphatase (ALP) activity and ALP staining

ALP activity and ALP staining assays were employed to evaluate the osteogenic differentiation of ADSC. For the ALP assay, ADSCs were seeded in 24 well plates at a density of 5×10^4 cells per well and cultured for 3 days. After the cells became adherent to the culture plate, GNPs were added to the osteogenic medium [DMEM supplemented with 10% FBS, 1% PS, 10 mM β-glycerol phosphate (Sigma-Aldrich), 0.1 μM dexamethasone (Sigma-Aldrich), and 300 μM ascorbic acid (Sigma-Aldrich)] at final concentration of 1, 5, and 14 μg/ml and cultured for 14 days. After incubation, the ADSCs were washed with DPBS and lysed with 1 × RIPA buffer (50 mM Tri-HCL, 150 mM NaCl, 0.25 % deoxycholic acid, 1 % NP-40 and 1 mM EDTA) with a protease inhibitor cocktail (Boehringer Mannheim GmbH, Germany) for 30 mins in ice. Each of the lysates was centrifuged at 1.3×10^4 rpm at 4 °C for 15 min to remove cell debris. After centrifugation, the supernatant was collected and then reacted with p-nitrophenol phosphate solution (pNPP, Sigma) in a 5 % CO_2 humidified incubator at 37 °C for 30 min. The reaction with pNPP was then stopped by adding 50 μl of 1 M NaOH. The level of p-nitrophenol production on the presence of ALPase was measured by absorption at 405 nm using a microplate reader. In order to evaluate the degree of osteogenic differentiation, cells were fixed in 3.7 % formaldehyde at RT for 10 min and then stained using an ALP staining kit (Sigma-Aldrich), according to manufacturer's instruction. After staining, the cell-seeded wells were washed twice with DPBS and observed by optical microscopy.

To confirm the effect of the Gel-GNP composite hydrogels, ADSCs were seeded on the various kinds of hydrogels at a density of 5×10^4 cells with osteogenic medium for 4, 7, 10, and 14 days. After incubation, the hydrogels were completely digested by treatment with 1 ml of 0.1% collagenase solution for 1 h, and the detached cells from each hydrogel were centrifuged for 5 min at 1500 rpm. Cell pellets were then lysed with 1 × RIPA buffer for 30 min in ice. After cell lysis, ALP activity and ALP staining were determined as described above.

Quantitative real-time polymerase chain reaction (Real-time PCR)

At each predetermined time period, the total RNA of ADSCs (seeded at a density of 5×10^4 cells) cultured on Gel, Gel-BMP, Gel-GNP **1**, **2**, and **3** was isolated by using an RNeasy Plus Mini Kit (Qiagen, CA, USA). According to manufacturer's instructions, 1 μg of total RNA was extracted from all specimens, and then transcribed into cDNA with AccuPower CycleScript RT Premix (Bioneer, Daejeon, Republic of Korea). The primers of the measured mRNA genes were as follows: bone sialoprotein (BSP) - 5′ – AAC GAA GAA AGC GAA GCA GAA – 3′ (sense) and 5′ – TCT GCC TCT GTG CTG TTG GT – 3′ (antisense), osteocalcin (OCN) - 5′- AGC AAA GGT GCA GCC TTT GT -3′ (sense) and 5′ – GCG CCT GGG TCT CTT CAC T -3′ (antisense), type I collagen (COL1) - 5′-ATG ACT ATG AGT ATG GGG AAG CA -3′ (sense) and 5′-TGG GTC CCT CTG TTA CAC TTT -3′ (antisense), runt-related transcription factor 2 (Runx2) - 5′- AAC CCA CGA ATG CAC TAT CCA -3′ (sense) and 5′- CGG ACA TAC CGA CGA GGG ACA TG -3′, and glyceraldehyde 3-phosphate dehydrogenase (GAPDH) - 5′ – ATG GGG AAG GTG AAG GTC G – 3′ (sense) and 5′ – GGG GTC ATT GAT GGC AAC AAT A – 3′ (antisense). Real-time PCR was analyzed by using iQ SYBR Green supermix (Bio-Rad, Hercules, CA, USA).

Threshold cycle values were calculated by using a comparative cycle threshold method. The fold change of the control group (Gel) at 7 days of culture was set as 1-fold and the ratio of the normalized fold change was calculated. Real-time PCR amplifications were carried out for 10 seconds at 95 ˚C, 30 seconds at 53 ~ 56 ˚C [bone sialoprotein (BSP) : 54 ˚C, osteocalcin (OCN) : 55 ˚C, collagen type I (COL1) : 53 ˚C, runt-related transcription factor 2 (RUNX2) : 56 ˚C] and 30 seconds at 72 ˚C for 45 cycles after the initial denaturation step of 10 minutes at 95 ˚C. All results were normalized by GAPDH.

In vivo animal model

6 male New Zealand rabbits (approximately 2.5 kg) were equally assigned into 6 groups: 1) blank (control), 2) Gel, 3) Gel-BMP, 4) Gel-GNP**1**, 5) Gel-GNP**2**, and 6) Gel-GNP**3**. Parietal bone defects with 10 mm in diameter were created on both the left and right side of the skull following previously described surgical procedures.[29] The defects were then filled with the prepared hydrogels. After 4 and 8 weeks to implantation, each rabbit was anesthetized, sacrificed, and the parietal bone was extracted. Micro computed tomography (μCT) examinations were used for assessment of bone healing in the bone defect. This was carried out by using a SkyScan1173 (SKYSCAN, Kartuizersweg 3B 2550 Kontich, Belgium) with the following settings: 130 kV voltage, 30 μA current, and 250 ms exposure time. The degree of bone healing on μCT was quantified by using the mean gray value and standard deviation of the region of interest (ROI). 3-dimensional images which had a total volume of the defect sites were obtained from μCT images by using On-demand software (CyberMed Inc., Korea).

Results

Preparation and characterization of Gel-GNP composite hydrogels

Prior to preparation of Gel-GNP composite hydrogels, an aqueous dispersion of GNPs was synthesized by citrate reduction. The morphology and size distribution of GNPs were observed by TEM and DLS. As shown in the TEM images (Fig. 2A), the synthesized GNPs were almost spherical and mono-dispersed with an average diameter of 27 ± 3 nm (Fig. 2B). GelMA is soluble in GNP solution and easily forms a Gel-GNP composite. The UV-vis spectra of the Gel-GNP composite showed a strong absorption at 530 nm due to the surface plasmon absorption of GNP (Fig. 2C), while no absorption was observed by the gelatin solution. Also, the maximum absorption of the 530 nm surface plasmon band was significantly increased when the amount of GNPs increases. The mixed solutions of GelMA and GNP were photo-cured by UV light. Fig. 2D shows the pictures of a pure Gel hydrogel and the photo-cross linked Gel-GNP hydrogel.

The presence of GNPs inside the hydrogel network was confirmed by thermal analysis. Fig. 3 shows the DSC and TGA curves of the Gel and Gel-GNP hydrogels. As shown in Fig. 3A, Gel hydrogel exhibits endothermic peaks at 202 °C and 325 °C due to the formation of cross-linked hydrogels. When GNPs are incorporated in the Gel hydrogel, their endothermic peaks were shifted to a different temperature or disappeared in the gained temperature range. Therefore, Gel-GNP hydrogel shows a new peak at 125 °C, this is due to the presence of GNPs in the

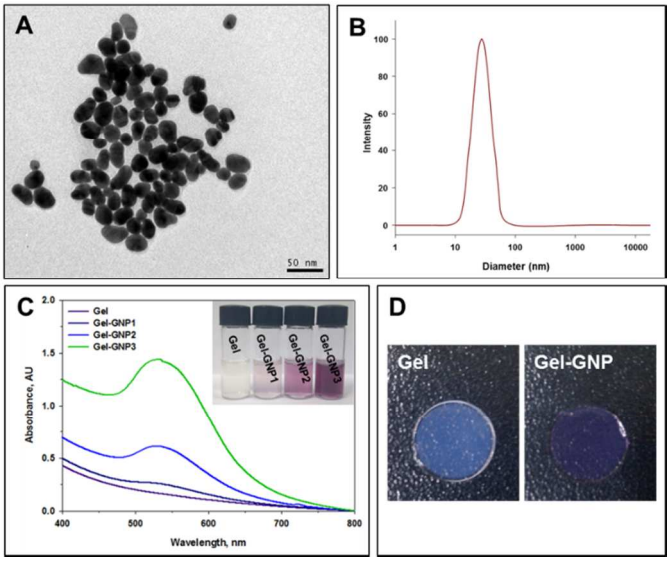

Fig. 2 Structure and characterization of GNP and Gel-GNP: (A) TEM images of GNP, (B) Size distribution of GNP, as measured by DLS, (C) Surface plasmon absorption of mixed solution with GNP and GelMA, (D) Photographs of photo-cured Gel and Gel-GNP.

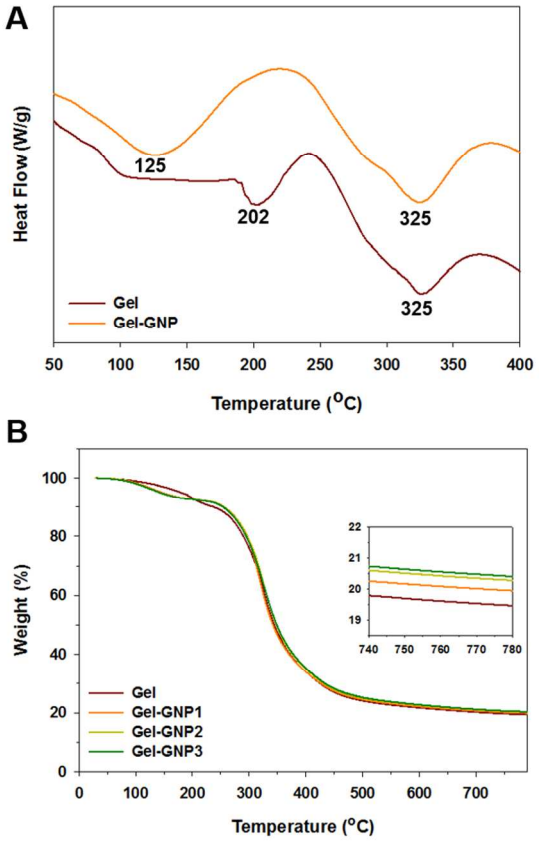

Fig. 3 (A) DSC thermograms of Gel and Gel-GNP and (B) TGA curves of Gel, Gel-GNP**1**, **2**, and **3**.

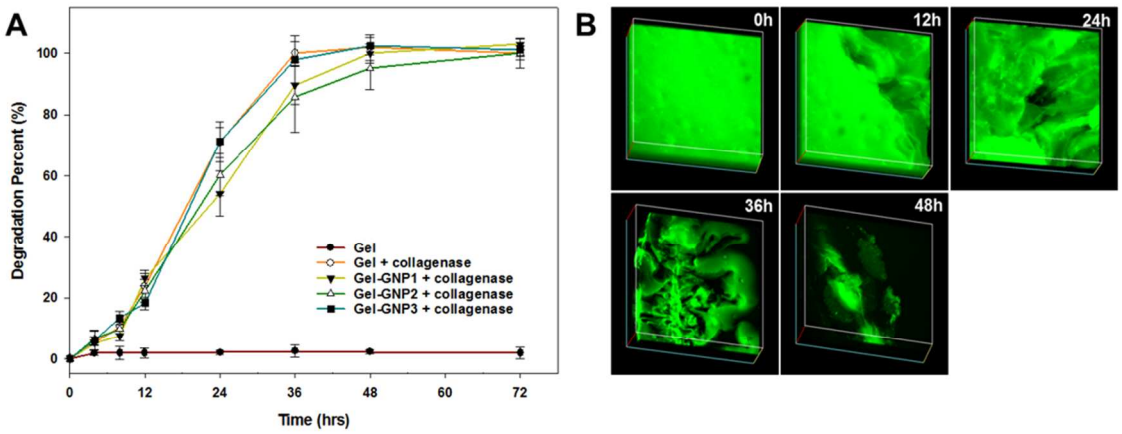

Fig. 4 (A) Enzymatic degradation rate by collagenase and (B) Morphological changes of Gel-GNP, as confirmed by CLSM.

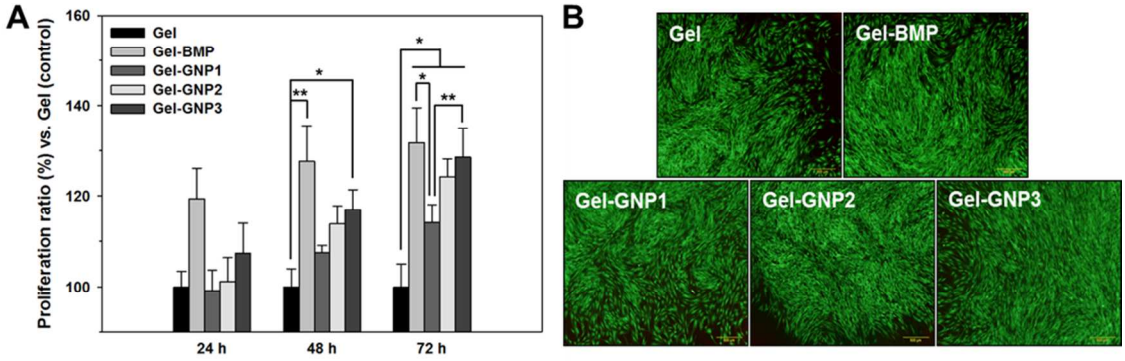

Fig. 5 Proliferation and viability of ADSCs cultured on Gel, Gel-BMP, Gel-GNP1, 2, and 3, investigated by CCK (A) and live/dead (B) assay. "*" indicates significant difference of p <0.05. "**" indicates significant difference of p <0.01.

hydrogel. TGA was performed to determine the percentage weight loss of Gel, Gel-GNP**1**, **2** and **3** (Fig. 3B). The thermal gravimetric curves show a feature between 250 °C and 500 °C, which indicates a large weight loss of all samples. This mass loss was due to the characteristic thermal behavior of gelatin.[30] The remaining mass of all samples as measured by TGA were approximately 19.46% (Gel), 19.94% (Gel-GNP**1**), 20.27% (Gel-GNP**2**) and 20.41% (Gel-GNP**3**) at 780 °C. The presence of GNP in the hydrogel was confirmed by this difference in decomposition between the Gel and Gel-GNP hydrogels.

After thermal testing of the Gel-GNP hydrogel network, the enzymatic degradation of the hydrogels was examined to confirm their enzymatic degradability. The degradation behaviors of the Gel and Gel-GNP hydrogels were determined by measuring weight loss. As shown in Fig. 4A, no significant weight changes in the Gel hydrogel were observed during 72 h when incubated without enzyme. In contrast, the Gel, Gel-GNP**1**, **2** and **3** hydrogels which were incubated with collagenase exhibited a significant decrease in mass over this time period. Fig. 4B shows the morphological changes of these fluorescently labeled hydrogels during *in vitro* degradation. There was a pronounced change in the hydrogel morphology upon incubation with collagenase which matches the results of the mass-loss experiment. These results indicated that the gelatin is a natural polymer derived from collagens and is susceptible to degrade by collagenase.

Effects of Gel-GNP hydrogels on the proliferation and viability of ADSCs

The cellular proliferation of ADSCs on the various hydrogels was determined by the CCK assay at different time intervals (Fig. 5A). Gel-BMP was used as a positive control and this material displayed ADSC proliferation levels of 19%, 27%, and 31% at 24, 48, and 72 h, respectively. Gel-GNP hydrogels exhibited a similar effect on proliferation of ADSCs. The proliferation rate of the cells increased as the GNP content in the hydrogels increased. In the case of the Gel-GNP**3**, the proliferation rate increased in a similar manner to the Gel-BMP and reached 28% in 72 h. The live/dead staining assay of the ADSCs showed similar results to the proliferation assay. This assay shows that the number of living cells was slightly increased with increased GNP load (Fig. 5B).

Effect of GNPs on the osteogenic differentiation of ADSCs

The effect of GNPs on the osteogenic differentiation was confirmed by measuring ALP activity and ALP staining (Fig. 6A). It was found that GNPs promoted the osteogenic differentiation of ADSCs in a dose-dependent manner at all tested concentrations of 1, 5, and 14 μg/ml. Also, there was a significant increase in the amount of stained ALP depositions at 10 days after GNP treatment (Fig. 6B).

Effect of Gel-GNP hydrogels on the osteogenic differentiation of ADSCs

The effect of Gel-GNP hydrogels on osteogenic differentiation was confirmed by measuring ALP activity (Fig. 7A). The ALP activity level of ADSCs on all specimens increased over the course of incubation. The level of ALP activity was significantly increased in the order of Gel, Gel-GNP**1**, **2**, **3**, and Gel-BMP. The Gel-GNP hydrogels exhibited a dose and time dependent effect on ALP activity. The highest dosed Gel-GNP**3** displayed a high ALP activity similar to Gel-BMP, which indicates that the Gel-GNP**3** can positively accelerate the osteogenic differentiation of ADSCs. As shown in Fig. 7B, it was visually confirmed that the amount of stained ALP depositions at 14 days of culture were increased in the order of Gel, Gel-GNP**1**, **2**, **3**, and Gel-BMP. Also, it was found that the amount of ALP deposited on Gel-GNP**3** and Gel-BMP were significantly higher than all the other specimens.

The mRNA expressions of various osteoblast gene markers, such as BSP, OCN, COL1, and Runx2 were determined by real-time PCR (Fig. 8). The results were normalized to GAPDH expression. As shown in Fig. 8A and B, the mRNA expressions of BSP and OCN, which is a late maker of osteogenic differentiation and mineralization process, were expressed at their lowest levels at 7 days of culture and then increased at 14 days in all specimens. The expression levels of these markers were significantly increased in the order of Gel, Gel-GNP**1**, **2**, **3**, and Gel-BMP. Among these specimens, Gel-BMP showed the highest mRNA expressions of BSP and OCN, and GNP-GNP**3** exhibited a similar effect with Gel-BMP. On the other hand, the mRNA expressions of COL1, which is an early marker of osteogenic maturation, was highest at 7 days and then decreased at 14 days in all specimens (Fig. 8C). The highest

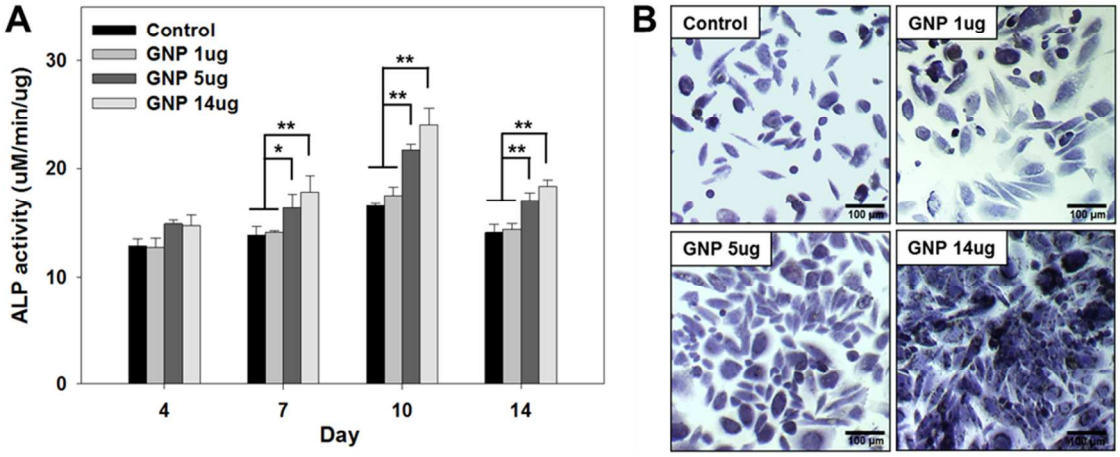

Fig. 6 ALP activity level (A) and ALP staining (B) of ADSCs cultured with GNPs. "*" indicates significant difference of p <0.05. "**" indicates significant difference of p <0.01.

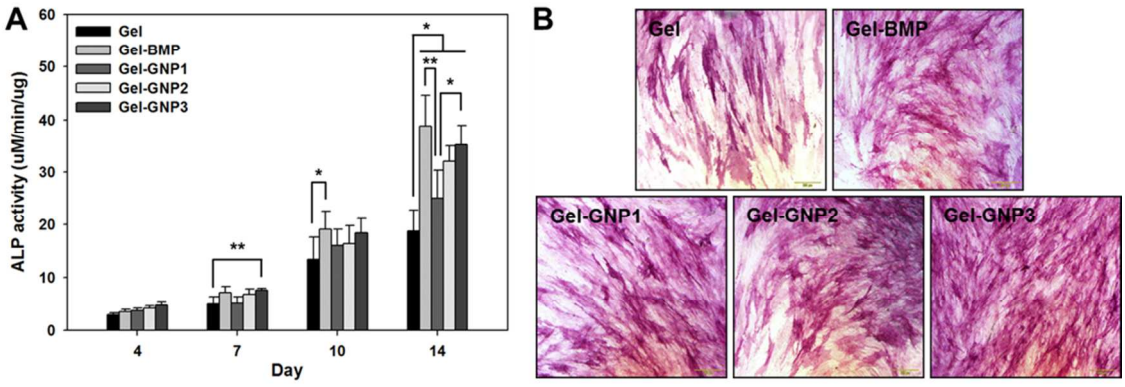

Fig. 7 ALP activity level (A) and ALP staining (B) of ADSCs cultured on Gel, Gel-BMP, Gel-GNP1, 2, and 3. "*" indicates significant difference of p <0.05. "**" indicates significant difference of p <0.01.

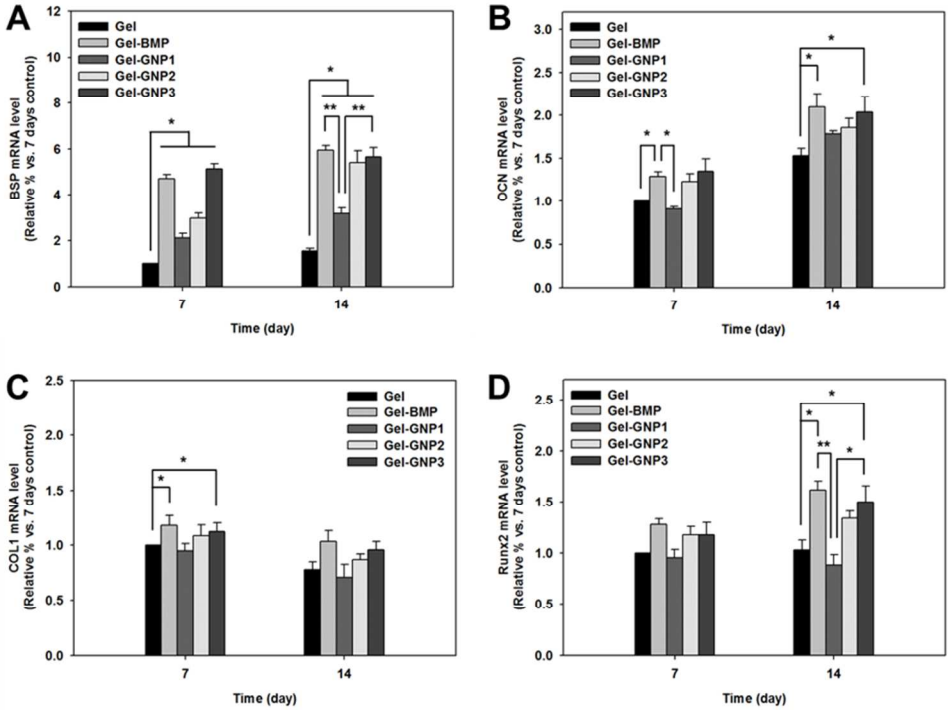

Fig. 8 Gene expressions of (A) BSP, (B) OCN, (C) COL1, and (D) Runx2 on Gel, Gel-GMP, Gel-GNP1, 2, and 3 at 7 and 14 days. "*" indicates significant difference of p <0.05. "**" indicates significant difference of p <0.01.

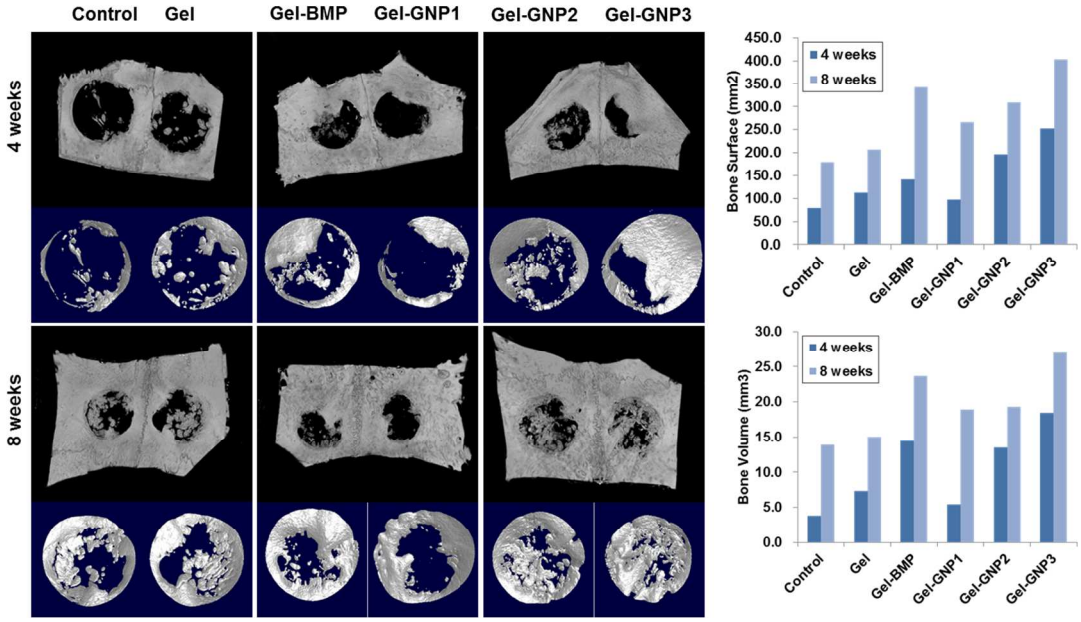

Fig. 9 3-dimensional scan images of rabbit calvaria after 4 and 8 weeks of implantation, and recovered bone area of the defected sites.

level of COL1 was observed with Gel-BMP and Gel-GNP**3** at each time interval. Another osteogenic transcription factor, Runx2, displayed an increased in all specimens over the course of time. The mRNA expression of Runx2 was significantly

increased in the order of Gel, Gel-GNP**1**, **2**, **3**, and Gel-BMP similar to the BSP and OCN results (Fig. 8D). In all markers, it was found that the mRNA expressions were increased in the order of Gel, Gel-GNP**1**, **2**, **3**, and Gel-BMP. In particular, Gel-GNP**3** showed a similar expression with Gel-BMP in all primers.

Effects of Gel-GNP hydrogels on bone regeneration *in vivo*

Parietal bone defects (10 mm diameter) were created by using previously described surgical procedures. The defect sites were filled with one of the five types of hydrogels (Gel, Gel-GMP, Gel-GNP**1**, **2**, and **3**). μCT analysis was performed at predetermined time points after surgery to confirm the bone healing effects of the various hydrogels. 3-dimensional images of the defected and regenerated sites were analyzed to obtain mean gray value of the ROI. As shown in Fig. 9, 3-dimensional images revealed that the total regenerated bone volume (RBV) of all groups increased between 4 and 8 weeks. It was found that all experimental groups (Gel, Gel-GMP, Gel-GNP**1**, **2**, and **3**) had a positive effect on bone healing in the defect sites as compared to the control group. A significant increase of RBV was identified in the site filled with Gel-BMP. Also, it was found that the level of RBV was significantly increased in the order of Gel-GNP**1**, **2**, and **3**. Gel-GNP hydrogels exhibited improved bone regeneration in a time- and dose-dependent manner.

Discussion

At the cellular level, GNPs can be useful as potential promoters of osteogenic differentiation. Previous reports have shown that GNPs enhance the ALP activity of MSCs and MC3T3-E1 osteoblast-like cells.[15,16] In this study, we used ADSCs to confirm the osteogenic effects of GNP loaded hydrogels. The preceding research analysis was necessary to investigate the effect of GNPs themselves on the osteogenic differentiation of ADSCs. The effect of GNPs on osteogenic differentiation of ADSCs in the presence of osteogenic medium was confirmed by measuring ALP activity, which is an early phenotypic marker for osteogenic differentiation of ADSCs. As shown in Fig. 6, it was found that the synthesized GNPs with an average diameter of 27 ± 3 nm effectively enhanced osteogenic differentiation by increasing ALP activity.

Based on this results, the hybrid hydrogel composed of gelatin and GNPs was designed and prepared to evaluate the capacity of this system to enhance osteogenic differentiation. Nanoparticles embedded into the hydrogel may be an excellent method to improve the functionality of the composite scaffold. The composite scaffolds with both polymeric and nano-sized materials also provides a proper surface roughness and good mechanical strength, which may enhance bone tissue regeneration.[31] Therefore, we selected photo-cured hydrogel due to its ease for incorporating and crosslinking with GNP. And gelatin was selected and applied as photo-cured hydrogel because it has several advantages including biocompatibility, non-toxicity after degradation, and possibility to introduce the photo-curable property.[32] The presence of GNPs inside the hydrogel network was confirmed by TGA and DSC (Fig. 3). It was found that the Gel-GNP system promoted the proliferation and viability (Fig. 5). Lee *et al.* described that the surface coated with gelatin nano gold composite lead to a good cell spreading ability and higher cell viability due to their increased roughness.[33] Interestingly, the Gel-GNP showed enhanced proliferation and viability of ADSC. These results are due to the presence of GNPs into hydrogel. In addition, Gel-GNP hydrogels promoted the osteogenic differentiation and mineralization of ADSCs similar to Gel-BMP (Fig. 7, and 8). Similar results were also reported that GNPs can enhance osteogenic differentiation *in vitro* condition.[15,16] However, previous researches just confirmed about their osteogenic effects at *in vitro* condition. It is difficult to fully recreate the complexity of *in vivo* system or provide desired results about the response of a physiological system using *in vitro* system.[34] The results of *in vitro* do not always concur with that of *in vivo*.[35] Therefore, we further confirmed the effectiveness of Gel-GNPs towards bone tissue regeneration using an animal model. The results of the μCT analysis agreed with the *in vitro* study results (Fig. 9). Also, these results indicate that GNP-GNP**3** exhibit a similar effect with Gel-BMP. The BMP family is made up of important growth factors which are critical for regenerating bone tissue. Among this family, BMP-2 has been widely used as a strong osteoinductive protein.[2,3,18] Although BMP-2 are beneficial effects on bone regeneration and repair, it has several disadvantage, including high cost, unwanted bone formation, and local inflammatory reaction.[19-21] Furthermore, a high BMP-2 concentration could lead to potential toxicity, apoptosis, immunogenic response, and cancer risks.[36] Therefore, it is necessary the development of alternative agents for bone tissue regeneration which provide less expensive, more safer, and osteogenic differentiation induction. GNPs are easy to synthesize from gold chloride to various types of GNPs at lab-scale.[11,12,37] The gold chloride, base material for making GNPs, provides relatively inexpensive price as compared with BMP-2. Also, GNPs showed no significant toxicity *in vivo*. Zhang et al found that 30 nm GNPs did not cause any significant damage of organs even though they accumulate in the liver, spleen, and kidney after intraperitoneal injection.[34] Therefore, GNP is suitable to use as an alternative material for BMP-2 in bone tissue regeneration.

The materials implanted in the defected bone tissue sites represent a feasible means to reconstruct and regenerate new bone tissue in damaged sites. Protein-based hydrogels work well for bone tissue regeneration due to their three-dimensional networks, tissue-like water content, and biodegradability.[2,3,29] The degradability of these materials is crucial to the formation and remodeling of mature tissue. Gel-GNP hydrogels are susceptible to local degradation via cell-secreted enzymes, and GNPs have absolutely no effect on their degradability (Fig. 4). This is due to the fact that gelatin is a naturally degradable polymer derived from collagens and is susceptible to hydrolysis by collagenase.[26,30] These results are important as when the cells attach and grow on the hydrogel, they should be capable of degrading the material via collagenase like enzymes. Thus biodegradable hydrogels have the potential to direct the migration, growth, and organization of cells during tissue regeneration.[38,39] Moreover, in our study, it was found that GNPs can be used as osteogenic promoters to stimulate osteogenic differentiation of ADSCs. When the Gel-GNP hydrogel networks are degraded by biological enzymes, the released GNP is delivered to the local region and accelerates new bone formation. Therefore, Gel-GNP is feasible for use as an implanted material in bone tissue regeneration.

Conclusions

In this study, we designed and prepared a novel hydrogel incorporating GNPs by photo-crosslinking. GNPs are attractive materials to use as osteogenic agents including less expense, non-toxicity, osteogenic differentiation induction. UV-induced

chemical crosslinking is an easy method to embed GNPs into the hydrogel. Therefore, Gel-GNP fabricated by photo-crosslinking have the both advantages of gelatin and GNPs. The synthesized GNPs have almost spherical and uniform shape with an average diameter of 27 ± 3 nm as confirmed by TEM and DLS. The presence of these GNPs in GelMA solution was confirmed by UV/Vis spectroscopy. The thermo-chemical properties of the hydrogels loaded with GNPs were confirmed by measuring DSC and TGA. It was found that Gel-GNPs are effectively degradable by biological interactions with collagenase. Cellular experiments show that the Gel-GNP promoted significantly higher ALP activity, proliferation, viability, and osteogenic differentiation of ADSCs. These results were similar to those obtained with Gel-BMP. Moreover, Gel-GNP displayed significantly higher new bone formation in animal tests. The results from in this study indicate that the Gel-GNP can be useful as an implant material in treating defected bone tissues.

Acknowledgements

This research was supported by the Public welfare & Safety research programthrough theNational Research Foundation of Korea (NRF) funded by the Ministry of Education, Science and Technology (NRF-2010-0019346), (NRF-2012-0008610), (NRF-2012R1A5A2051388), and by Bio-industry Technology Development Program(312062-5) of iPET(Korea Institute of Planning and Evaluation for Technology in Food, Agriculture, Forestry and Fisheries), Ministry for Food, Agriculture, Forestry and Fisheries, Republic of Korea.

References

1 T. Hirakura, K. Yasugi, T. Nemoto, M. Sato, T. Shimoboji, Y. Aso, N. Morimoto and K. Akiyoshi, *J. Control. Release.*, 2010, **142**, 483-489.
2 Y. I. Chung, K. M. Ahn, S. H. Jeon, S. Y. Lee, J. H. Lee and G. Tae, *J. Control. Release.*, 2007, **121**, 91-99.
3 K. H. Park, H. Kim, S. Moon and K. Na, *J. Biosci. Bioeng.*, 2009, **108**, 530-537.
4 T. Jayaramudu, G. M. Raghavendra, K. Varaprasad, R. Sadiku and K. M. Raju, *Carbohydr. Polym.*, 2013, **92**, 2193-2200.
5 V. R. Babu, C. Kim, S. Kim, C. Ahn and Y. I. Lee, *Carbohydr. Polym.*, 2010, **81**, 196-202.
6 M. B. Mohamed, T. S. Ahmadi, S. Link, M. Braun and M. A. El-Sayed, *Chem. Phys. Lett.*, 2001, **343**, 55-63.
7 P. B. Malafaya, G. A. Silva and R. L. Reis, *Adv. Drug Deliv. Rev.*, 2007, **59**, 207-233.
8 A. S. Hoffman, *Adv. Drug Deliv. Rev.*, 2002, **54**, 3-12.
9 A. Veis and J. Cohen, *Nature*, 1960, **186**, 720-721.
10 Y. Takagishi, T. Kawakami, Y. Hara, M. Shinkai, T. Takezawa and T. Nagamune, *Tissue Eng.*, 2006, **12**, 927-937.
11 D. A. Giljohann, D. S. Seferos, W. L. Daniel, M. D. Massich, P. C. Patel and C. A. Mirkin, *Angew. Chem. Int. Ed.*, 2010, **49**, 3280-3294.
12 L. Dykman and N. Khlebtsov, *Chem. Soc. Rev.*, 2012, **41**, 2256-2282.
13 E. Boisselier and D. Astruc, *Chem. Soc. Rev.*, 2009, **38**, 1759-1782.
14 R. A. Sperling, P. Rivera Gil, F. Zhang, M. Zanella and W. J. Parak, *Chem. Soc. Rev.*, 2008, **37**, 1896-1908.
15 C. Yi, D. Liu, C. C. Fong, J. Zhang and M. Yang, *ACS Nano*, 2010, **4**, 6439-6448.
16 D. D. Liu, J. C. Zhang, C. Q. Yi and M. S. Yang, *Chinese Sci. Bull.*, 2010, **55**, 1013-1019.
17 O. J. Sul, J. C. Kim, T. W. Kyung, H. J. Kim, Y. Y. Kim, S. H. Kim, J. S. Kim and H. S. Choi, *Biosci. Biotechnol. Biochem.*, 2010, **74**, 2209-2213.
18 P. C. Bessa, M. Casal and R. L. Reis, *J. Tissue Eng. Regen. Med.*, 2008, **2**, 81-96.
19 D. Benglis, M. Y. Wang and A. D. Levi, *Neurosurgery*, 2008, **62**, ONS423-431.
20 S. C. McGovern, W. Fong and J. C. Wang, *Spine*, 2010, **35**, 1655-1659.
21 H. K. Kim, I. Oxendine and N. Kamiya, *Bone*, 2013, **54**, 141-150.
22 J. Gimble and F. Guilak, *Cytotherapy*, 2003, **5**, 362-369.
23 B. M. Strem, K. C. Hicok, M. Zhu, I. Wulur, Z. Alfonso, R. E. Schreiber, J. K. Fraser and M. H. Hedrick, *Keio J. Med.*, 2005, **54**, 132-141.
24 J. W. Nichol, S. T. Koshy, H. Bae, C. M. Hwang, S. Yamanlar and A. Khademhosseini, *Biomaterials*, 2010, **31**, 5536-5544.
25 H. Aubin, J. W. Nichol, C. B. Hutson, H. Bae, A. L. Sieminski, D. M. Cropek, P. Akhyari and A. Khademhosseini, *Biomaterials*, 2010, **31**, 6941-6951.
26 C. B. Hutson, J. W. Nichol, H. Aubin, H. Bae, S. Yamanlar, S. Al-Haque, S. T. Koshy and A. Khademhosseini, *Tissue Eng. Part A*, 2011, **17**, 1713-1723.
27 D. N. Heo, D. H. Yang, H. J. Moon, J. B. Lee, M. S. Bae, S. C. Lee, W. J. Lee, I. C. Sun and I. K. Kwon, *Biomaterials*, 2012, **33**, 856-866.
28 M. S. Bae, J. E. Kim, J. B. Lee, D. N. Heo, D. H. Yang, J. H. Kim, K. R. Kwon, J. B. Bang, H. Bae and I. K. Kwon, *Carbohydr. Polym.*, 2013, **92**, 167-175.
29 M. S. Bae, D. H. Yang, J. B. Lee, D. N. Heo, Y.D Kwon, I. C. Youn, K. Choi, J. H. Hong, G. T. Kim, Y. S. Choi, E. H. Hwang and I. K. Kwon, *Biomaterials*, 2011, **32**, 8161-8171.
30 S. E. Kim, D. N. Heo, J. B. Lee, J. R. Kim, S. H. Park, S. H. Jeon and I. K. Kwon, *Biomed. Mater.*, 2009, **4**, 044106.
31 K. Kim and J. P. Fisher, *J. Drug. Target.*, 2007, **15**, 241-252.
32 K. Peters, A. Salamon, S. V. Vlierberghe, J. Rychly, M. Kreutzer, H. Neumann, E. Schacht and P. Dubruel, *Adv. Eng. Mater.*, 2009, **11**, B155-B161.
33 Y. H. Lee, G. Bhattarai, S. Aryal, N. H. Lee, M. H. Lee, T. G. Kim, E. C. Jhee, H. Y. Kim and H. K. Yi, *Appl. Suf. Sci.*, 2010, **256**, 5882-5887.
34 X. D. Zhang, D. Wu, X. Shen, P. X. Liu, N. Yang, B. Zhao, H. Zhang, Y. M. Sun, L. A. Zhang and F. Y. Fan, *Int. J. Nanomedicine*, 2011, **6**, 2071-2081.
35 C. M. Sayes, A. A. Marchione, K. L. Reed and D. B. Warheit, *Nano Lett.*, 2007, **7**, 2399-2406.
36 S. Gitelis, R. M. Wilkins, A. W. Yasko, *AAOS NOW*, 2008, **2**, 31.
37 R. Willson, Chem. Soc. Rev., 2008, **37**, 2028-2045.
38 A. Khademhosseini, G. Eng, J. Yeh, J. Fukuda, J. Blumling, R. Langer, J. A. Burdick, *J. Biomed. Mater. Res. A*, 2006, **79**, 522-532.
39 H. Qi, Y. Du, L. Wang, H. Kaji, H. Bae, A. Khademhosseini, *Adv. Mater.*, 2010, **22**, 5276-5281.